BIOCHEMISTRY
including biophysical chemistry & molecular biology

Article

pubs.acs.org/biochemistry

Water Networks in Fast Proton Transfer during Catalysis by Human Carbonic Anhydrase II

Rose Mikulski,[†] Dayne West,[‡] Katherine H. Sippel,[‡] Balendu Sankara Avvaru,[‡] Mayank Aggarwal,[‡] Chingkuang Tu,[†] Robert McKenna,*[,‡] and David N. Silverman*[,†,‡]

[†]Department of Pharmacology and [‡]Department of Biochemistry and Molecular Biology, University of Florida, Gainesville, Florida 32610, United States

Supporting Information

ABSTRACT: Variants of human carbonic anhydrase II (HCA II) with amino acid replacements at residues in contact with water molecules in the active-site cavity have provided insights into the proton transfer rates in this protein environment. X-ray crystallography and ^{18}O exchange measured by membrane inlet mass spectrometry have been used to investigate structural and catalytic properties of variants of HCA II containing replacements of Tyr7 with Phe (Y7F) and Asn67 with Gln (N67Q). The rate constants for transfer of a proton from His64 to the zinc-bound hydroxide during catalysis were 4 and 9 μs^{-1} for Y7F and Y7F/N67Q, respectively, compared with a value of 0.8 μs^{-1} for wild-type HCA II. These higher values observed for Y7F and Y7F/N67Q HCA II could not be explained by differences in the values of the pK_a of the proton donor (His64) and acceptor (zinc-bound hydroxide) or by the orientation of the side chain of the proton shuttle residue His64. They appeared to be associated with a reduced level of branching in the networks of hydrogen-bonded water molecules between proton shuttle residue His64 and the zinc-bound solvent molecule as observed in crystal structures at 1.5−1.6 Å resolution. Moreover, Y7F/N67Q HCA II is unique among the variants studied in having a direct, hydrogen-bonded chain of water molecules between the zinc-bound solvent and N$^{\epsilon}$ of His64. This study provides the clearest example to date of the relevance of ordered water structure to rate constants for proton transfer in catalysis by carbonic anhydrase.

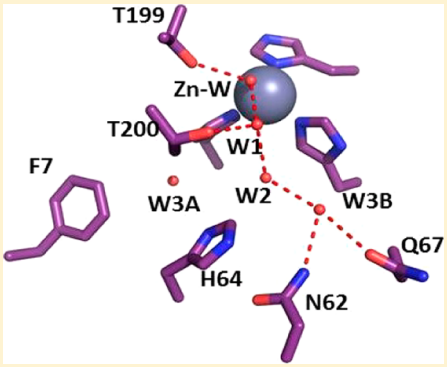

The carbonic anhydrases (CAs) are primarily zinc metalloenzymes that rapidly hydrate carbon dioxide to form bicarbonate and a proton. The well-studied α class includes the mammalian CAs with roles in acid−base balance, fluid secretion, respiration, and other physiological processes.[1] Humans are known to express many CA isozymes throughout the body,[1,2] including the structurally and kinetically well characterized human carbonic anhydrase II (HCA II).[3−5] The first stage of catalysis is the binding of bicarbonate to zinc followed by the dehydration of bicarbonate (eq 1). The second stage is the transfer of a proton from buffer in solvent BH^+ to proton shuttle His64 and subsequently to zinc-bound hydroxide to regenerate the catalytic zinc-bound water (eq 2).

$$EZnH_2O + HCO_3^- \overset{-H_2O}{\rightleftharpoons} EZnHCO_3^- \rightleftarrows EZnOH^- + CO_2 \quad (1)$$

$$\text{His64-}EZnOH^- + BH^+ \rightleftarrows H^+\text{His64-}EZnOH^- + B \rightleftarrows \text{His64-}EZnH_2O + B \quad (2)$$

The intramolecular transfer of a proton from His64 to the zinc-bound hydroxide in the second stage of the catalysis (eq 2) is as fast as 1 μs^{-1} and is rate-limiting for the maximal velocity of HCA II.[6,7] The position of the side chain of His64 is observed in inward and outward orientations (Figure 1); in the inward orientation, the imidazole ring of His64 is ~7.5 Å from

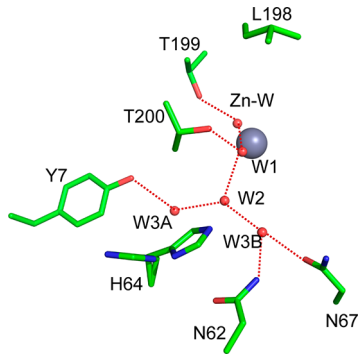

Figure 1. Active site of wild-type HCA II from the crystal structure at pH 8.0 (PDB entry 2ili).[8] The zinc ion and the oxygen of water molecules are shown as gray and red spheres, respectively. The water network of the active site is labeled W1, W2, etc. Dashed red lines are assumed hydrogen bonds. The side chain of proton shuttle His64 is shown in both the inward and outward orientations. This figure was generated and rendered with PyMOL (http://www.pymol.org).

Received: August 14, 2012
Revised: November 7, 2012
Published: December 6, 2012

 © 2012 American Chemical Society

Table 1. Crystal Structure Data and Refinement Statistics for N67Q and Y7F/N67Q HCA II

	N67Q	Y7F/N67Q
wavelength (Å)	1.5418	1.5418
space group	$P2_1$	$P2_1$
unit cell parameters [a, b, c (Å); β (deg)]	42.0, 41.2, 72.1; 104.3	42.1, 41.2, 71.9; 104.5
total no. of reflections	35820	31729
redundancy	3.6 (2.5)[d]	3.8 (3.6)[d]
completeness (%)	97.7 (80.5)[d]	99.7 (99.8)[d]
resolution (Å)	50.0−1.50 (1.55−1.50)[d]	50.0−1.60 (1.66−1.60)[d]
R_{sym}[a]	7.3 (38.9)[d]	8.4 (47.3)[d]
$I/\sigma(I)$	14.5 (4.1)[d]	13.1 (2.8)[d]
R_{cryst}[b] (%)	18.5	16.6
R_{free}[c] (%)	21.4	20.5
range of amino acid residues	3−261	3−261
no. of protein atoms	2180	2199
no. of H_2O molecules	376	319
rmsd for bond lengths (Å)	0.006	0.006
rmsd for bond angles (deg)	1.086	1.019
Ramachandran statistics (%) (most favored, allowed, outlier)	87.6, 12.4, 0.0	86.6, 13.4, 0.0
average B factor (Å^2) (main chain, side chain, Zn, solvent)	18.2, 21.4, 11.5, 29.6	19.8, 22.0, 10.5, 28.7

[a] $R_{sym} = \sum|I - \langle I\rangle|/\sum\langle I\rangle$. [b] $R_{cryst} = (\sum||F_o| - |F_c||/\sum|F_o|) \times 100$. [c] R_{free} is calculated in same manner as R_{cryst}, except that it uses 5% of the reflection data omitted from refinement. [d] Values in parentheses represent data for the highest-resolution bin.

the zinc.[8−10] An ordered, hydrogen-bonded network of water molecules extending between the zinc-bound water and His64 is observed in crystal structures of HCA II (Figure 1) and is believed to offer clues about the pathway for intramolecular proton transfer during catalysis.[3−5]

The water network in HCA II appears to form hydrogen bonds with hydrophilic residues lining the active-site cavity and is branched at the water molecule labeled W2 in Figure 1. A number of studies have replaced residues in the active-site cavity, which alters the structure of the water network, and introduced changes in the orientation of His64 and the pK_a of its imidazole ring[11−13] to determine the relevance of the observed water structure to the rate constants for proton transfer. One significant observation is that the variant of HCA II with Tyr7 replaced with Phe (Y7F) has an enhanced rate constant of intramolecular proton transfer 5-fold greater than that of the wild type and less branching of the water network connecting His64 and the zinc-bound solvent.[11] Computational studies indicate that the rate of proton transfer is expected to be faster in unbranched water chains.[14,15]

In this work, we have constructed the Y7F/N67Q HCA II variant that has a water network showing less branching than in the wild type. It also has a completed hydrogen-bonded water chain and a shorter distance between His64 and the zinc-bound solvent as determined from the crystal structure at 1.6 Å resolution. The appropriate single mutants Y7F and N67Q are also examined. For the double mutant, the rate constant for intramolecular proton transfer at 9.0 μs^{-1} is 10-fold greater than that of the wild type measured by ^{18}O exchange. This allows a more complete understanding of the factors that influence proton transfer through water chains in a protein environment. HCA II serves as a simple model for examining proton transfers in more complex systems such as the photosynthetic reaction center, bacteriorhodopsin, and cytochrome c oxidase.

MATERIALS AND METHODS

Enzymes. Variants of HCA II were made with the QuickChange II Site-Directed Mutagenesis Kit (Agilent) on the expression vector encoding full-length wild-type HCA II. The entire region encoding HCA II was determined for each mutant to confirm the correct DNA sequence. Plasmids were transformed for expression into *Escherichia coli* BL21(DE3)-pLysS cells (Agilent). The transformed cells were grown in LB medium to which 1.0 mM $ZnSO_4$ had been added and induced with 1.0 mM IPTG when the OD_{600} reached 0.6. Each variant was purified by affinity chromatography using *p*-(aminomethyl)benzenesulfonamide coupled to agarose beads (Sigma).[16] The concentration of HCA II and variants was determined by titration of active sites by the tight-binding inhibitor ethoxzolamide while the activity was being measured by the ^{18}O method.

^{18}O Exchange. The catalysis of HCA II has been well studied by measuring the exchange of ^{18}O from labeled bicarbonate and CO_2 species to water using membrane inlet mass spectrometry.[17] The method is based on the depletion of ^{18}O from CO_2 that passes across the membrane inlet into a mass spectrometer (Extrel EXM-200). The apparatus allows a continuous measurement of the isotopic content of CO_2 under controlled conditions in solution. The initial step of the catalysis by HCA II is the dehydration of labeled bicarbonate with a probability of leaving a ^{18}O-labeled hydroxide at the zinc (eq 3). The second step involves the protonation of the zinc-bound hydroxide subsequently releasing $H_2{}^{18}O$, which is very greatly diluted by $H_2{}^{16}O$ in solution (eq 4).

$$\begin{aligned} &HCOO^{18}O^- + EZnH_2O \rightleftarrows EZnHCOO^{18}O^- \\ &\rightleftarrows COO + EZn^{18}OH^- \end{aligned} \quad (3)$$

$$\begin{aligned} &H + His64\text{-}EZn^{18}OH^- \overset{H_2O}{\rightleftharpoons} His64\text{-}EZnH_2{}^{18}O \\ &\rightarrow His64\text{-}EZnH_2O + H_2{}^{18}O \end{aligned} \quad (4)$$

The ^{18}O exchange method allows a rate for both steps of the catalysis to be determined.[17] The rate of the first step, exchange between CO_2 and HCO_3^- at chemical equilibrium, is designated R_1 and is described by eq 5. The maximal rate constant of the conversion between CO_2 and HCO_3^- is k_{cat}^{ex}; the apparent binding constant for binding of the substrate to

dx.doi.org/10.1021/bi301099k | *Biochemistry* 2013, 52, 125−131

the enzyme is K_{eff}^{S}, and [S] is the concentration of the substrate, either CO_2 or bicarbonate, for the hydration or dehydration direction.[18] The k_{cat}^{ex}/K_{eff}^{S} ratio is in principle and practice equivalent to k_{cat}/K_m determined in steady-state experiments.[18]

$$R_1/[E] = (k_{cat}^{ex}[CO_2])/(K_{eff}^{CO_2} + [CO_2]) \quad (5)$$

The rate of the second step, the transfer of a proton and release of water in eq 4, is termed R_{H_2O}. R_{H_2O} is interpreted in terms of a rate constant k_B for the transfer of a proton to the zinc-bound hydroxide (eq 6). The ionization constants of the proton donor and the zinc-bound water molecule are given in eq 6 as $(K_a)_{donor}$ and $(K_a)_{ZnH_2O}$, respectively.

$$R_{H_2O}/[E] = k_B/\{[1 + (K_a)_{donor}/[H^+]][1 + [H^+]/(K_a)_{ZnH_2O}]\} \quad (6)$$

The uncatalyzed and carbonic anhydrase- catalyzed ^{18}O exchange at chemical equilibrium was measured in the absence of buffer at a total substrate concentration (all CO_2 species) of 25 mM using membrane-inlet mass spectrometry.[17] Reactions were conducted at 10 and 25 °C as noted, and the total ionic strength of the solution was maintained at 0.2 M by the addition of Na_2SO_4. The determination of the kinetic and ionization constants of eqs 5 and 6 was conducted by nonlinear least-squares methods (Enzfitter, Biosoft).

Crystallography. Crystals of mutants N67Q and Y7F/N67Q HCA II were obtained using the hanging drop method.[19] The crystallization drops were prepared by mixing 5 μL of protein [concentration of ~15 mg/mL in 100 mM Tris-HCl (pH 8.0)] with 5 μL of the precipitant solution [1.25 M sodium citrate and 100 mM Tris-Cl (pH 8.0)] against a well of 1000 μL of the precipitant solution. Crystals were observed within a week at 293 K.

The N67Q and Y7F/N67Q HCAII crystals were flash-cooled after a soak in cryoprotectant, 30% glycerol with the precipitant solution, before being mounted. The X-ray data were obtained at 100 K using an R-AXIS V++ optic system from Viarimax HR and a Rigaku RU-H3R Cu rotating anode operating at 50 kV and 100 mA. The detector−crystal distance was set to 80 mm. The oscillation steps were 1° with a 6 min exposure per image for 360°. Data set statistics for the crystals are listed in Table 1.

The model building was done manually with Coot,[20] and refinement was conducted with the PHENIX suite.[21] The starting phasing model was the wild-type HCA II structure of Fisher et al.[22] (PDB entry 1tbt) with the waters removed and the mutated residues as well as His64 changed to Ala to reduce model bias.

RESULTS

Catalysis. The pH dependence of catalysis of the hydration of CO_2 determined by ^{18}O exchange was determined for each of variants Y7F, N67Q, and Y7F/N67Q HCA II. The data for Y7F HCA II were reported previously.[11] Profiles of $R_1/[E]$ over a range of pH values were obtained, and eq 5 was used to determine the catalytic constants $k_{cat}^{ex}/K_{eff}^{CO_2}$ for hydration of CO_2 (Figure 2). The ionic strength was maintained at 0.2 M using Na_2SO_4, and the substrate was $NaHCO_3$; the pH was adjusted with dilute H_2SO_4, and no buffers were added. Fits to a single ionization appear to be satisfactory except at very low pH values of <6 where the data showed decreased values for $k_{cat}^{ex}/K_{eff}^{CO_2}$ possibly because of additional ionizations or denaturation. This was particularly apparent in the variants

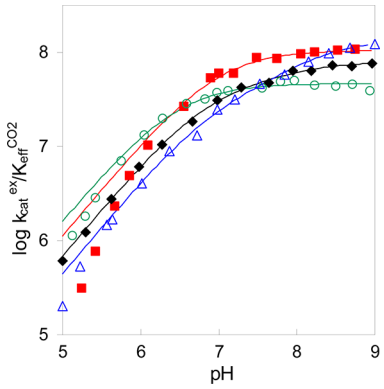

Figure 2. pH profiles for $k_{cat}^{ex}/K_{eff}^{CO_2}$ (M^{-1} s^{-1}) for the hydration of CO_2 catalyzed by (◆) wild-type HCA II, (○) N67Q HCA II, (△) Y7F HCA II, and (■) Y7F/N67Q HCA II. Data were obtained by ^{18}O exchange between CO_2 and water using solutions containing all species of CO_2 at 25 mM and sufficient Na_2SO_4 to maintain an ionic strength of 0.2 M.

containing the Y7F replacement, as already noted for Y7F HCA II.[11] The maximal pH-independent values of $k_{cat}^{ex}/K_{eff}^{CO_2}$ are compared in Table 2; these are similar, with values between 50

Table 2. Maximal Values of Rate Constants for Hydration of CO_2 and Proton Transfer in Dehydration Catalyzed by HCA II and Variants

enzyme	$k_{cat}^{ex}/K_{eff}^{CO_2}$ for CO_2 hydration (μM^{-1} s^{-1})[a]	k_B for proton transfer (μs^{-1})[b]
wild type	120	0.80
Y7F[c]	120	3.9
N67Q	50	1.7
Y7F/N67Q[d]	80	9.0

[a]Measured from the exchange of ^{18}O between CO_2 and water in the hydration direction (eq 5). Derived for each variant by a fit of the data (as in Figure 2) to a single ionization. The standard errors for these rate constants are generally ≤15%. [b]Measured from the exchange of ^{18}O between CO_2 and water (as in Figure 3) using eq 6 in the dehydration direction. The standard errors are ≤22%. [c]Data at 10 °C from ref 11. [d]Data at 10 °C.

and 120 μM^{-1} s^{-1}. The pK_a values of the zinc-bound water, pK_{aZnH_2O}, determined from the fits to a single ionization obtained from the pH profiles of $k_{cat}^{ex}/K_{eff}^{CO_2}$ (Table 3, column 2) are also quite similar. These similarities reflect the distances of these residues from the zinc: 7.0 Å between the hydroxyl oxygen of Tyr7 and the zinc and 8.4 Å between the carboxamide carbon of Asn67 and the zinc.

Table 3. Values of Apparent pK_a Obtained by Kinetic Measurements of Catalysis by HCA II and Variants

enzyme	pK_{aZnH_2O}[a]	pK_{aZnH_2O}[b]	pK_{aHis64}[b]
wild type	6.9	6.8	7.2
Y7F[c]	7.1	7.0	6.0
N67Q	6.5	6.7	6.6
Y7F/N67Q[d]	6.9	6.3	6.2

[a]Measured from a fit of the data of Figure 2 to a single ionization. The standard errors in pK_a are mostly ±0.1 and no greater than ±0.2. [b]Measured from the fits of eq 6 to the data in Figure 3. The values of pK_a have standard errors no greater than ±0.2. [c]These data at 10 °C from ref 11. [d]These data at 10 °C.

dx.doi.org/10.1021/bi301099k | Biochemistry 2013, 52, 125−131

The advantage of the ^{18}O exchange method is that catalysis by variants of CA can be examined in solutions without added buffer to determine rates of intermolecular proton transfer. Experiments conducted at steady state do not have this advantage and must use external buffers to control pH. The rate constant $R_{H_2O}/[E]$ measures the second stage of catalysis in which rate-limiting intermolecular proton transfer releases $H_2{}^{18}O$ from the active site (eq 4). The pH profiles of $R_{H_2O}/[E]$ for each mutant were predominantly bell-shaped (Figure 3), reflecting the transfer of a proton from the imidazolium side

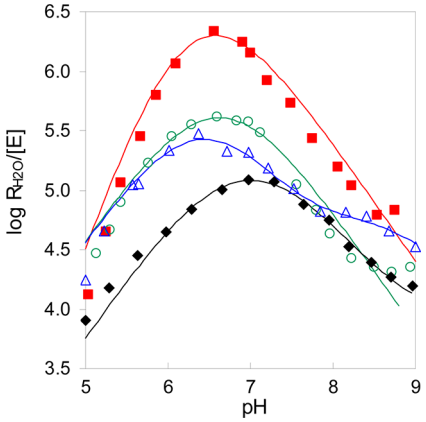

Figure 3. pH profiles for $R_{H_2O}/[E]$ (s^{-1}), the proton transfer-dependent rate of release of ^{18}O-labeled water catalyzed by (◆) wild-type HCA II, (○) N67Q HCA II, (△) Y7F HCA II, and (■) Y7F/N67Q HCA II. Conditions were as described in the legend of Figure 2.

chain of His64 to the zinc-bound hydroxide.[23] The bell-shaped curves were fit to eq 6 to yield a rate constant of proton transfer, k_B. The range of k_B values was approximately 10-fold (Table 2). Because the values of pK_a were nearly identical for the proton donor (His64) and acceptor, there was no issue in the assignment of these values. The exception is Y7F HCA II in which the pK_a of the zinc-bound water was confirmed by measurement of the esterase activity.[11]

Crystallography. The crystal structures of variants N67Q and Y7F/N67Q of HCAII were determined to 1.5−1.6 Å resolution using data that had a completeness of >92% (Figures 4 and 5). Figure S1 of the Supporting Information shows the omit maps with electron densities. The crystal structure data and refinement statistics are listed in Table 1. Overall, no major structural perturbations were observed; the rmsd for C^{α} atoms was 0.1 Å for both variants when they were compared to wild-type HCA II (PDB entry 2ili[8]). The proton shuttle residue His64 has been shown to occupy two conformations in wild-type HCA II, inward and outward with respect to the orientation in the active-site cavity.[8,10] The outward conformation was dominant in N67Q HCA II, while the inward conformation was observed in Y7F/N67Q HCA II, similar to the Y7F variant previously published.[11] Coordinates for N67Q HCA II and Y7F/N67Q HCA II have been deposited in the Protein Data Bank as entries 3TVN and 4IDR, respectively.

Compared with wild-type HCA II, the hydrogen-bonded solvent network in the active-site cavity was mostly conserved for the three variants of HCA II depicted in Figures 1, 4, and 5. However, there were distinct differences. In the case of Y7F, the water molecule labeled W3A was not observed (Figure 5).[11] For Y7F/N67Q HCA II, W3A was observed but was not within

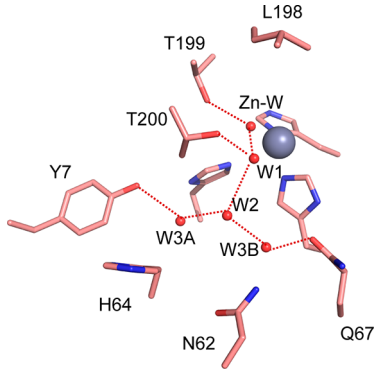

Figure 4. Active-site structure for N67Q HCA II crystallized at pH 8.0. The three histidine residues (His94, His96, and His119) coordinating the zinc (gray sphere) are not labeled. The oxygen atoms of water molecules identified in the active-site cavity are shown as red spheres and labeled W1, W2, etc. Presumed hydrogen bonds are represented as dashed red lines. This figure was generated and rendered using PyMOL.

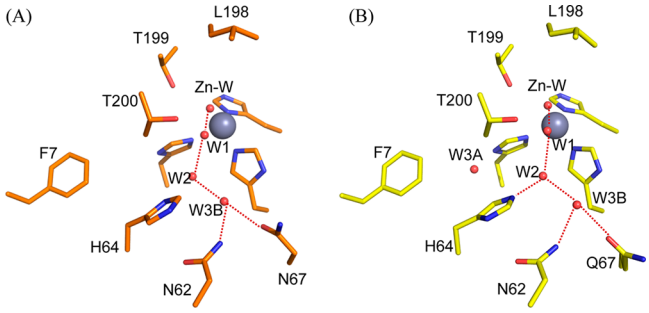

Figure 5. Comparison of active-site structures for variants of HCA II crystallized at pH 8.0: (A) Y7F HCA II (PDB entry 2nxt[11]) and (B) Y7F/N67Q HCA II. This diagram was constructed as described in the legend of Figure 4.

hydrogen bonding distance of W2; moreover, the distance between W3B and W2 (3.1 Å) was longer than in the wild type (2.7 Å) (Table 4). In addition, in Y7F/N67Q, the distance

Table 4. Comparison of Distances (angstroms) in the Proposed Hydrogen Bond Network Determined from the Crystal Structures of Variants of HCA II

	wild type	Y7F[a]	Y7F/N67Q	N67Q
Zn solvent−W1	2.7	2.7	2.7	2.7
W1−W2	2.7	2.6	2.6	2.9
W2−W3A	2.8	not available	4.3	2.9
W2−W3B	2.7	2.6	3.1	2.4
W2−H64[b]	3.2/6.3	3.2	2.9	6.7
Zn solvent−H64[b]	7.2/10.0	7.1	6.7	10.5
H64	in/out	in	in	out

[a]These data from ref 11. [b]For Y7F and N67Q the distance is from N^{δ}, but for Y7F/N67Q the distance is from N^{ε} because the imidazole ring is flipped.

between W2 and N^{δ} of His64 (2.9 Å) is shorter and hence indicates a stronger hydrogen bond than in the wild type for which His64 is inward (3.2 Å) (Table 4). This is also reflected in the respective distances between the zinc-bound solvent and N^{ε} of His64 (Table 4). The carboxamide group of the Gln substitution at residue 67 extended farther into the active-site cavity than the Asn residue it replaced. For N67Q, an

dx.doi.org/10.1021/bi301099k | Biochemistry 2013, 52, 125−131

associated effect was an increase in the distance from the zinc-bound solvent to N^{δ} of His64 (10.5 Å, outward orientation) compared with that of the wild type [10.0 Å, outward (Table 4)].

DISCUSSION

These catalytic and structural results for variants of HCA II with amino acid replacements at residues in contact with water molecules in the active-site cavity provide insight into the proton transfer rates in this protein environment. The rate constant k_B of 9 μs^{-1} for the transfer of a proton from His64 to the zinc-bound hydroxide in catalysis by Y7F/N67Q HCA II (Table 2) is the fastest measured for a variant of this isozyme. The previously studied Y7F HCA II was also found to have rapid proton transfer with a k_B of 4 μs^{-1}.[11] The value for wild-type HCA II is 0.8 μs^{-1} (Table 2).[11]

These high k_B values observed for Y7F and Y7F/N67Q HCA II were not explained by differences in the values of the pK_a between the proton donor (His64) and acceptor (zinc-bound hydroxide). This is shown in Table 3 in which the values of pK_a are similar for these variants. Moreover, previous reports showed that the pH dependence of k_B is rather flat in the vicinity of ΔpK_a ($pK_{aZnH_2O} - pK_{aHis64}$) near zero.[24,25] We can comment, however, that the increments in the rate constant for proton transfer, k_B, caused by the replacements at residues 7 and 67 are additive in nature, as illustrated in a double-mutant cycle (Scheme S1 of the Supporting Information).[26]

In the cases of Y7F and Y7F/N67Q HCA II, the enhanced rate constants are associated with a predominant inward orientation of the His64 side chain in the crystal structures (Figure 5). However, the orientation of His64 in crystal structures has not been shown to affect the rate constant for proton transfer according to the following data. Variant N62L has His64 predominantly inward and N67L predominantly outward with other aspects of their protein structure nearly identical, yet their values of k_B are the same, 0.2 μs^{-1}.[11,12,27] The same conclusion that the inward and outward conformations in crystal structures of His64 do not influence the proton transfer rate was reached using a mutant in which Thr200 was substituted with Ser.[28] This is supported by computational studies that suggest that the orientation of His64 need not influence this intramolecular proton transfer rate.[29,30]

It remains then to examine the solvent structure observed in the active site. Although these low-energy networks of ordered water are observed in crystal structures and are taken as significant clues about the proton transfer pathway, clusters of hydrogen-bonded water in the active-site cavity in solution have lifetimes typically in the picosecond range.[31] Comparison of the crystal structures of the variants of Table 2 and other reports of variants of HCA II[11,12,32] shows that the two most efficient enzymes in proton transfer, Y7F and Y7F/N67Q HCA II, have less branched water structure; specifically, water molecule W3A is not observed in Y7F and is not within hydrogen bonding distance of the water chain in Y7F/N67Q (Figure 5 and Table 4). Furthermore, in Y7F/N67Q, there is a long and weak hydrogen bond between W2 and W3B compared with that in the wild type (Figure 5 and Table 4). We also point out that this double mutant is unique among the variants of HCA II we have examined in that it shows a normal hydrogen bond length between W2 and N^{ε} of His64; other variants show this as a very weak hydrogen bond at best (Table 4). Thus, Y7F/N67Q has the most completely formed hydrogen-bonded chain of unbranched water molecules between the zinc-bound solvent and N^{ε} of His64 among the variants examined (Table 4). Computations show that proton transfer through an unbranched, hydrogen-bonded water network is more rapid than through a branched pathway.[14,15,33] This feature of a more direct pathway in the structures of Y7F and Y7F/N67Q HCA II appears to be most relevant in explaining the proton transfer efficiencies of these variants.

When catalysis was measured by stopped-flow spectrophotometry, the steady-state constants k_{cat} for dehydration were close in magnitude for the wild type (0.24 μs^{-1}) and Y7F/N67Q (0.19 μs^{-1}), as were the values of k_{cat} for hydration (Table S1 of the Supporting Information). The steady-state constant k_{cat} measures many steps in either the dehydration or hydration direction, among which are conversion of bound substrate to product, product dissociation, intramolecular proton transfer, and possibly proton transfer steps between buffer in solution and zinc-bound hydroxide via His64. At steady state, enzyme species are not necessarily at equilibrium concentrations, and the enzyme species preceding a rate-limiting step accumulates above equilibrium concentrations. The solvent H/D kinetic isotope effects on k_{cat} for hydration of CO_2 catalyzed by wild-type and Y7F/N67Q CA II are near 3.2 for both enzymes measured in the presence of excess buffer (Table S1 of the Supporting Information). This indicates that proton transfer is a predominant rate-contributing step for both the wild type and variant measured at steady state.

The ^{18}O exchange rate for proton transfer, R_{H_2O}, from which we obtain k_B is determined at chemical equilibrium and focuses more on proton transfer because it contains many fewer steps of the catalysis than k_{cat}. In the ^{18}O exchange experiment, there is no buffer in solution, and because there is relatively little proton transfer between the enzyme and solution, there is no need for His64 to change orientation to sustain catalysis. These features provide an explanation for why k_B is greater than k_{cat}. The results are consistent with the influence of the structure of the specific water chains through which proton transfer occurs. In view of the many potential proton transfer pathways that have been found in CA II,[34] the data reflect the different proton transfer pathways involved in the equilibrium and steady-state experiments that result in different rate constants.

This study with the greatly enhanced proton transfer of Y7F/N67Q HCA II provides the clearest example to date of the relevance of the ordered water structure to rate constants for proton transfer in catalysis by carbonic anhydrase. The complement of these studies with the pertinent computational results of rapid proton transfer through unbranched water chains[14,15,31] is gratifying. It appears that the arrays of ordered, hydrogen-bonded water molecules as observed in crystal structures provide relevant information to explain efficient intramolecular proton transfer in carbonic anhydrase.

ASSOCIATED CONTENT

Supporting Information

A table of steady-state constants for the hydration of CO_2 and dehydration of bicarbonate catalyzed by wild-type and Y7F/N67Q HCA II and a double-mutant cycle for the values of k_B for catalysis by the enzymes of Table 2. This material is available free of charge via the Internet at http://pubs.acs.org.

dx.doi.org/10.1021/bi301099k | Biochemistry 2013, 52, 125−131

AUTHOR INFORMATION

Corresponding Author

*D.N.S.: Department of Pharmacology, College of Medicine, University of Florida, Box 100267, Gainesville, FL 32610; phone, (352) 392-3556; fax, (352) 392-9696; e-mail, silvrmn@ufl.edu. R. McKenna: Department of Biochemistry and Molecular Biology, College of Medicine, University of Florida, Box 100245, Gainesville, FL 32610; phone, (352) 392-5696; fax, (352) 392-3422; e-mail, rmckenna@ufl.edu.

Funding

This work was supported by National Institutes of Health Grant GM25154.

Notes

The authors declare no competing financial interest.

ABBREVIATIONS

N67Q HCA II, variant of human carbonic anhydrase II in which Asn67 was replaced with Gln; AE, anion exchange protein; PDB, Protein Data Bank; rmsd, root-mean-square deviation.

REFERENCES

(1) Chegwidden, W. R., Carter, N. D., and Edwards, Y. H. (2000) *The Carbonic Anhydrases: New Horizons*, Birkhauser Verlag, Basel, Switzerland.

(2) Supuran, C. T., Scozzafava, A., and Conway, J. (2004) *Carbonic Anhydrase: Its Inhibitors and Activators*, CRC Press, Boca Raton, FL.

(3) Silverman, D. N., and McKenna, R. (2007) Solvent-Mediated Proton Transfer in Catalysis by Carbonic Anhydrase. *Acc. Chem. Res. 40*, 669−675.

(4) Christianson, D. W., and Fierke, C. A. (1996) Carbonic anhydrase: Evolution of the zinc binding site by nature and by design. *Acc. Chem. Res. 29*, 331−339.

(5) Lindskog, S. (1997) Structure and mechanism of carbonic anhydrase. *Pharmacol. Ther. 74*, 1−20.

(6) Khalifah, R. G. (1971) Carbon Dioxide Hydration Activity of Carbonic Anhydrase. 1. Stop-Flow Kinetic Studies on Native Human Isoenzyme-B and Isoenzyme-C. *J. Biol. Chem. 246*, 2561−2573.

(7) Steiner, H., Jonsson, B. H., and Lindskog, S. (1975) Catalytic Mechanism of Carbonic-Anhydrase: Hydrogen-Isotope Effects on Kinetic-Parameters of Human C Isoenzyme. *Eur. J. Biochem. 59*, 253−259.

(8) Fisher, S. Z., Maupin, C. M., Budayova-Spano, M., Govindasamy, L., Tu, C., Agbandje-McKenna, M., Silverman, D. N., Voth, G. A., and McKenna, R. (2007) Atomic crystal and molecular dynamics simulation structures of human carbonic anhydrase II: Insights into the proton transfer mechanism. *Biochemistry 46*, 2930−2937.

(9) Liljas, A., Lovgren, S., Bergsten, P. C., Carlbom, U., Petef, M., Waara, I., Strandbe, B., Fridborg, K., Jarup, L., and Kannan, K. K. (1972) Crystal Structure of Human Carbonic Anhydrase-C. *Nat. New Biol. 235*, 131−137.

(10) Nair, S. K., and Christianson, D. W. (1991) Unexpected pH-Dependent Conformation of His-64, the Proton Shuttle of Carbonic Anhydrase-II. *J. Am. Chem. Soc. 113*, 9455−9458.

(11) Fisher, S. Z., Tu, C. K., Bhatt, D., Govindasamy, L., Agbandje-McKenna, M., McKenna, R., and Silverman, D. N. (2007) Speeding up proton transfer in a fast enzyme: Kinetic and crystallographic studies on the effect of hydrophobic amino acid substitution in the active site of human carbonic anhydrase II. *Biochemistry 46*, 3803−3813.

(12) Zheng, J. Y., Avvaru, B. S., Tu, C., McKenna, R., and Silverman, D. N. (2008) Role of Hydrophilic Residues in Proton Transfer during Catalysis by Human Carbonic Anhydrase II. *Biochemistry 47*, 12028−12036.

(13) Jackman, J. E., Merz, K. M., Jr., and Fierke, C. A. (1996) Disruption of the active site solvent network in carbonic anhydrase II decreases the efficiency of proton transfer. *Biochemistry 35*, 16421−16428.

(14) Cui, Q., and Karplus, M. (2003) Is a "proton wire" concerted or stepwise? A model study of proton transfer in carbonic anhydrase. *J. Phys. Chem. B 107*, 1071−1078.

(15) Maupin, C. M., Saunders, M. G., Thorpe, I. F., McKenna, R., Silverman, D. N., and Voth, G. A. (2008) Origins of enhanced proton transport in the Y7F mutant of human carbonic anhydrase II. *J. Am. Chem. Soc. 130*, 11399−11408.

(16) Khalifah, R. G., Strader, D. J., Bryant, S. H., and Gibson, S. M. (1977) C-13 Nuclear Magnetic-Resonance Probe of Active-Site Ionizations in Human Carbonic-Anhydrase B. *Biochemistry 16*, 2241−2247.

(17) Silverman, D. N. (1982) Carbonic anhydrase: Oxygen-18 exchange catalyzed by an enzyme with rate-contributing proton-transfer steps. *Methods Enzymol. 87*, 732−752.

(18) Simonsson, I., Jonsson, B. H., and Lindskog, S. (1979) C-13 NMR study of carbon dioxide-bicarbonate exchange catalyzed by human carbonic anhydrase-C at chemical-equilibrium. *Eur. J. Biochem. 93*, 409−417.

(19) McPherson, A. (1982) *Preparation and Analysis of Protein Crystals*, Wiley, New York.

(20) Otwinowski, Z., and Minor, W. (1997) Processing of X-ray Diffraction Data Collected in Oscillation Mode. *Methods Enzymol. 276*, 307−326.

(21) Adams, P. D., Afonine, P. V., Bunkoczi, G., Chen, V. B., Davis, I. W., Echols, N., Headd, J. J., Hung, L. W., Kapral, G. J., Grosse-Kunstleve, R. W., McCoy, A. J., Moriarty, N. W., Oeffner, R., Read, R. J., Richardson, D. C., Richardson, J. S., Terwilliger, T. C., and Zwart, P. H. (2010) PHENIX: A comprehensive Python-based system for macromolecular structure solution. *Acta Crystallogr. D66*, 213−221.

(22) Fisher, Z., Hernandez Prada, J. A., Tu, C., Duda, D., Yoshioka, C., An, H., Govindasamy, L., Silverman, D. N., and McKenna, R. (2005) Structural and kinetic characterization of active-site histidine as a proton shuttle in catalysis by human carbonic anhydrase II. *Biochemistry 44*, 1097−1105.

(23) Tu, C. K., Silverman, D. N., Forsman, C., Jonsson, B. H., and Lindskog, S. (1989) Role of histidine 64 in the catalytic mechanism of human carbonic anhydrase II studied with a site-specific mutant. *Biochemistry 28*, 7913−7918.

(24) An, H., Tu, C., Duda, D., Montanez-Clemente, I., Math, K., Laipis, P. J., McKenna, R., and Silverman, D. N. (2002) Chemical rescue in catalysis by human carbonic anhydrases II and III. *Biochemistry 41*, 3235−3242.

(25) Silverman, D. N., Tu, C., Chen, X., Tanhauser, S. M., Kresge, A. J., and Laipis, P. J. (1993) Rate-equilibria relationships in intramolecular proton transfer in human carbonic anhydrase III. *Biochemistry 32*, 10757−10762.

(26) Mildvan, A. S., Weber, D. J., and Kuliopulos, A. (1992) Quantitative Interpretations of Double Mutations of Enzymes. *Arch. Biochem. Biophys. 294*, 327−340.

(27) Mikulski, R. L., and Silverman, D. N. (2010) Proton transfer in catalysis and the role of proton shuttles in carbonic anhydrase. *Biochim. Biophys. Acta 1804*, 422−426.

(28) Krebs, J. F., Fierke, C. A., Alexander, R. S., and Christianson, D. W. (1991) Conformational Mobility of His-64 in the Thr200Ser Mutant of Human Carbonic Anhydrase-II. *Biochemistry 30*, 9153−9160.

(29) Riccardi, D., Konig, P., Guo, H., and Cui, Q. (2008) Proton transfer in carbonic anhydrase is controlled by electrostatics rather than the orientation of the acceptor. *Biochemistry 47*, 2369−2378.

(30) Shimahara, H., Yoshida, T., Shibata, Y., Shimizu, M., Kyogoku, Y., Sakiyama, F., Nakazawa, T., Tate, S., Ohki, S. Y., Kato, T., Moriyama, H., Kishida, K., Tano, Y., Ohkubo, T., and Kobayashi, Y. (2007) Tautomerism of histidine 64 associated with proton transfer in catalysis of carbonic anhydrase. *J. Biol. Chem. 282*, 9646−9656.

(31) Maupin, C. M., McKenna, R., Silverman, D. N., and Voth, G. A. (2009) Elucidation of the Proton Transport Mechanism in Human Carbonic Anhydrase II. *J. Am. Chem. Soc. 131*, 7598−7608.

(32) Domsic, J. F., Williams, W., Fisher, S. Z., Tu, C., Agbandje-McKenna, M., Silverman, D. N., and McKenna, R. (2010) Structural and Kinetic Study of the Extended Active Site for Proton Transfer in Human Carbonic Anhydrase II. *Biochemistry 49*, 6394−6399.
(33) Wu, Y., and Voth, G. A. (2003) A computer simulation study of the hydrated proton in a synthetic proton channel. *Biophys. J. 85*, 864−875.
(34) Roy, A., and Taraphder, S. (2010) Role of protein motions on proton transfer pathways in human carbonic anhydrase II. *Biochim. Biophys. Acta 1804*, 352−361.